Pathogenic T cells have a paradoxical protective effect in murine autoimmune diabetes by boosting Tregs

Yenkel Grinberg-Bleyer,[1,2,3] David Saadoun,[1,2,3] Audrey Baeyens,[1,2,3] Fabienne Billiard,[1,2,3] Jérémie D. Goldstein,[1,2,3] Sylvie Grégoire,[1,2,3] Gaëlle H. Martin,[1,2,3] Rima Elhage,[1,2,3] Nicolas Derian,[1,2,3] Wassila Carpentier,[1,4] Gilles Marodon,[1,2,3] David Klatzmann,[1,2,3] Eliane Piaggio,[1,2,3] and Benoît L. Salomon[1,2,3]

[1]Université Pierre et Marie Curie — Univ Paris 06, [2]CNRS UMR 7211, [3]INSERM U959, Paris, France.
[4]Plate-forme Post-Génomique P3S, Hôpital Pitié-Salpêtrière, Paris, France.

CD4+CD25+Foxp3+ Tregs play a major role in prevention of autoimmune diseases. The suppressive effect of Tregs on effector T cells (Teffs), the cells that can mediate autoimmunity, has been extensively studied. However, the in vivo impact of Teff activation on Tregs during autoimmunity has not been explored. In this study, we have shown that CD4+ Teff activation strongly boosts the expansion and suppressive activity of Tregs. This helper function of CD4+ T cells, which we believe to be novel, was observed in the pancreas and draining lymph nodes in mouse recipients of islet-specific Teffs and Tregs. Its physiological impact was assessed in autoimmune diabetes. When islet-specific Teffs were transferred alone, they induced diabetes. Paradoxically, when the same Teffs were cotransferred with islet-specific Tregs, they induced disease protection by boosting Treg expansion and suppressive function. RNA microarray analyses suggested that TNF family members were involved in the Teff-mediated Treg boost. In vivo experiments showed that this Treg boost was partially dependent on TNF but not on IL-2. This feedback regulatory loop between Teffs and Tregs may be critical to preventing or limiting the development of autoimmune diseases.

Introduction

The peripheral T cell repertoire of any individual contains autoreactive T cells specific for a variety of self antigens (1). Their activation could induce an autoimmune process, eventually leading to an autoimmune disease. Severe and prolonged inflammation in a tissue may lead to the activation of pathological autoreactive T cells by several mechanisms (2, 3). At the site of inflammation or in draining LNs, tissue damage results in an enhanced presentation of autoantigens by newly recruited mature antigen-presenting cells. Also, released cytokines, chemokines, and inflammatory factors may attract and induce bystander activation of autoreactive memory/effector T cells (Teffs), leading to initiation or exacerbation of a preexisting autoimmune process and eventually clinical disease.

These potentially pathologic processes are controlled by several factors and feedback mechanisms. For example, strongly activated Teffs can secrete the antiinflammatory IL-10 cytokine (4). Also, IFN-γ expression by Teffs may favor production of the antiinflammatory indoleamine 2,3-dioxygenase (5) or promote Tim-3/galectin-9 interaction regulating T helper type 1 immunity (6). But one of the major mechanisms controlling inflammation and autoreactive Teffs involves the CD4+CD25+Foxp3+ Tregs (7–12). Moreover, high numbers of Tregs are observed in inflamed tissues in various contexts (13–19). Different mechanisms may explain this increased Treg frequency. A Treg subset with an "activated/memory" phenotype preferentially migrates to inflamed tissues (20). Also, enhanced presentation of autoantigens by increased num-

bers of mature DCs in inflamed tissues may favor the activation of autoreactive Tregs (21–23), which would then turn on their suppressive activity and exert bystander suppression (24, 25).

Thus, during an autoimmune process, there is a local enrichment of both autoreactive Teffs and Tregs. Since the efficacy of Treg-mediated suppression depends on the equilibrium between activated Teffs and activated Tregs (26), any factor that could tip this balance to one side or the other could then determine the outcome of the autoimmune process. In this study, we have identified what we believe is a novel feedback mechanism, which may help maintain this equilibrium. We hypothesized that in order to maintain a Teff/Treg balance, in addition to the well-established suppressive activity of Tregs on Teffs, there could be a feedback mechanism allowing Teffs to boost Treg activity. We indeed found that antigen-specific activation of Teffs boosts Treg expansion and improves their suppressive function. Thus, diabetogenic Teffs paradoxically help islet-specific Tregs to provide sustained protection from diabetes.

Results

Teffs boost Treg activation during an autoimmune response. Tregs proliferate in vivo when stimulated by their cognate antigen (21, 27–29). In this report, we addressed whether activated conventional CD4+ T cells would have an impact on the level of Treg activation in vivo in an autoimmune context. This was first studied in a model of adoptive transfer of influenza virus HA-specific (transgenic) Tregs and Teffs into ins-HA transgenic mice, which express HA under the control of the insulin promoter. We had previously observed that HA-specific Tregs (HA-Tregs) preferentially proliferated and expanded at days 5–7 after transfer in draining pancreatic LNs (PLNs) of ins-HA homozygous mice (29). When we repeated the experiment in ins-HA hemizygous recipients, which express lower
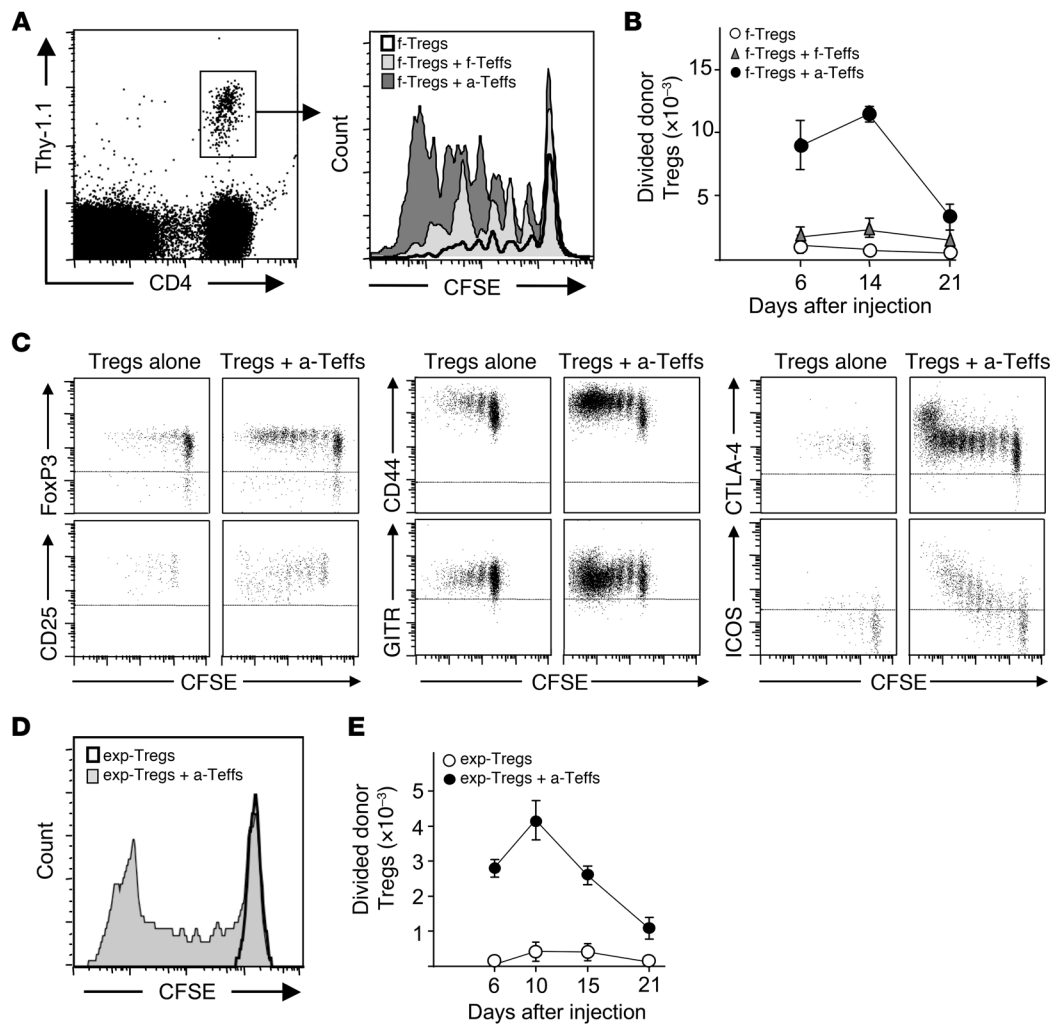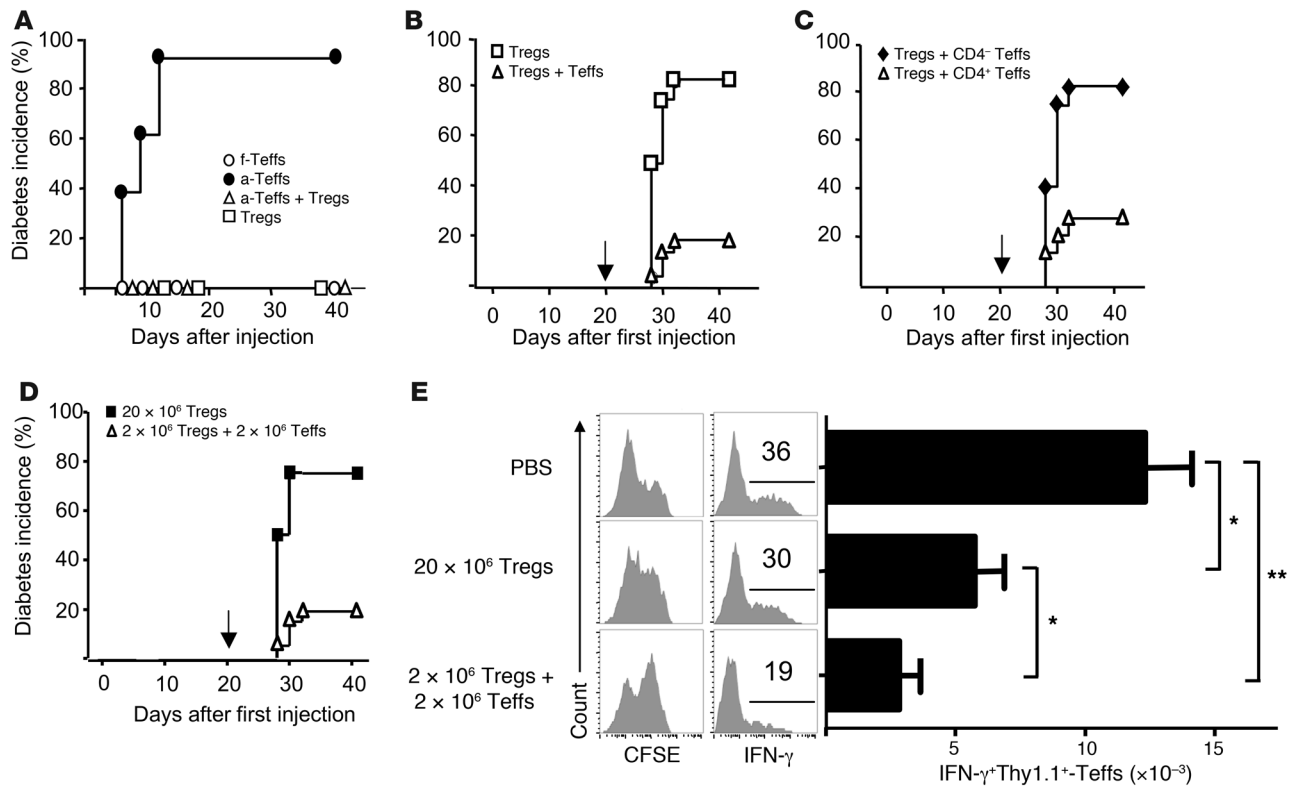
Figure 1
Islet-specific Teffs strongly boost the activation of islet-specific Tregs. (**A–C**) Ins-HA mice were injected with CFSE-labeled Thy-1.1+ freshly purified HA-Tregs alone (f-Tregs) or were cotransferred with freshly purified HA-Teffs (f-Tregs + f-Teffs) or preactivated HA-Teffs (f-Tregs + a-Teffs). (**A**) Representative CFSE profile of donor Tregs (gated on CD4+Thy-1.1+ cells as shown in the left panel) in PLNs 14 days after cell injection. (**B**) Absolute number of divided donor Tregs (CFSEdimCD4+Thy-1.1+ cells) were quantified in PLNs at 6, 14, and 21 days after cell transfer. The graph shows mean data from 3 to 8 mice per time point pooled from 4 independent experiments. (**C**) Representative expression of the indicated proteins on donor Tregs in PLNs 7 days after cell injection. Plots, gated on CD4+Thy-1.1+ cells (for FoxP3) or CD4+Thy-1.1+FoxP3+ cells (for the other markers), are representative of 2 to 5 independent experiments. Horizontal dashed lines delineate positive staining. (**D** and **E**) Ins-HA mice were injected with CFSE-labeled Thy-1.1+ expanded HA-Tregs alone (exp-Tregs) or were cotransferred with preactivated HA-Teffs (exp-Treg + a-Teffs). (**D**) Representative CFSE profile of donor Tregs in PLNs 10 days after cell injection. (**E**) Absolute numbers of divided donor Tregs (CFSEdimCD4+Thy-1.1+ cells) were quantified in PLNs various days after cell injection. The graph shows mean data from 4 to 8 mice per time point collected from 4 independent experiments. Error bars represent SD.

levels of HA in β cells (30), HA-Tregs proliferated at a lower level and were detected in PLNs for 3 weeks (Figure 1). We then assessed whether coadministration of HA-Teffs had an effect on HA-Treg activation (Figure 1). The cotransfer of freshly purified HA-specific T cells induced a moderate but marked increase of proliferation and expansion of donor Tregs. Strikingly, the cotransfer of preactivated HA-specific T cells (HA-Teffs) induced a strong increase in proliferation of donor Tregs over the 3-week duration of the experiment, with a 6- to 17-fold increase in the absolute number of divided HA-Tregs at days 6 to 21 in PLNs (Figure 1, A and B). In this Teff-dependent Treg boost (Teff→Treg boost), divided HA-Tregs maintained high expression of FoxP3, glucocorticoid-

induced TNFR-related protein (GITR), and CTLA-4, decreased CD25 expression, and upregulated CD44 expression, consistent with an "effector-memory" Treg phenotype (20, 29, 31). Interestingly, the expression of inducible T cell costimulator (ICOS) molecule was strongly upregulated upon division during the Teff→Treg boost (Figure 1C). No Treg expansion was observed in nondraining LNs. Control preactivated Teffs specific for a nonself antigen that were not reactivated in PLNs after transfer in ins-HA mice did not boost activation of coinjected HA-Treg (data not shown). Thus, activated islet-specific Teffs strongly boosted the expansion of islet-specific Tregs, which acquired an activated phenotype at the site of Ag presentation.
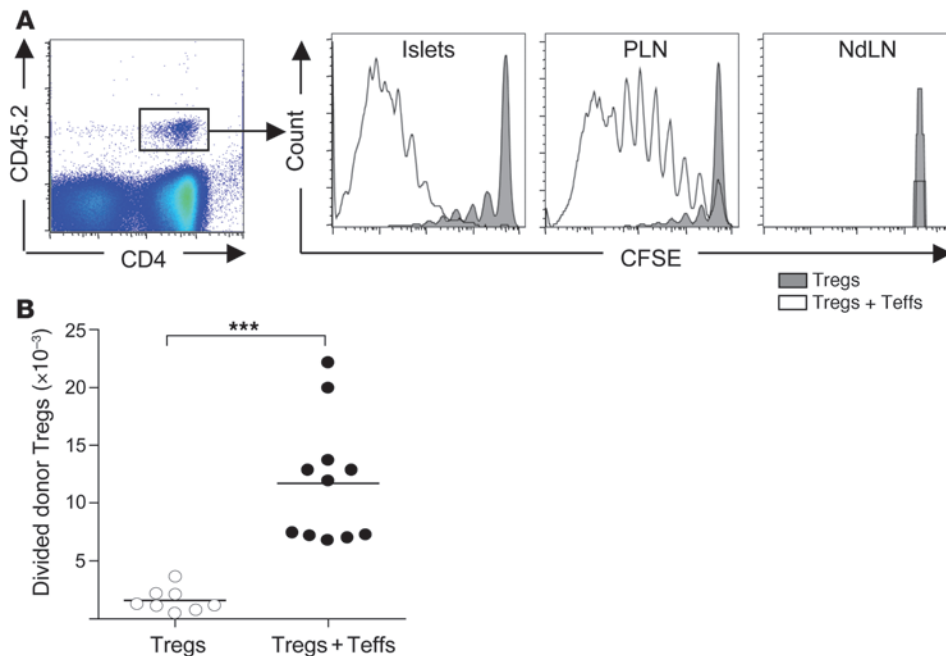
Figure 2
Paradoxical protective effect of diabetogenic T cells in autoimmune diabetes. (**A**) Diabetes incidence in ins-HA mice after transfer of freshly purified HA-Teffs (white circles, $n = 13$) or preactivated HA-Teffs (black circles, $n = 9$) or expanded HA-Tregs (white squares) or coinjection of preactivated HA-Teffs and expanded HA-Tregs (white triangles, $n = 9$). Data were from 4 experiments. (**B**) Ins-HA mice were transferred with expanded HA-Tregs alone (white squares, $n = 12$) or with preactivated HA-Teffs (white triangles, $n = 21$). 3 weeks later (arrow), mice were challenged for diabetes induction with preactivated HA-Teffs. Data were from 4 independent experiments. (**C**) Ins-HA mice were cotransferred with expanded HA-Tregs and the CD4$^+$ (white triangles, $n = 14$) or CD4$^-$ (black diamonds, $n = 12$) fractions of preactivated HA-Teffs. Mice were challenged 3 weeks later (arrow) with preactivated HA-Teffs. Data were from 2 independent experiments. (**D** and **E**) Ins-HA mice were transferred with 20×10^6 expanded HA-Tregs alone (black squares, $n = 4$) or coinjected with 2×10^6 expanded HA-Tregs and 2×10^6 preactivated HA-Teffs (white triangles, $n = 21$) or injected with PBS only (for **E**). Mice were challenged 3 weeks later with preactivated HA-Teffs to test their susceptibility to diabetes induction (**D**) or with CFSE-labeled Thy-1.1$^+$ preactivated HA-Teffs to analyze their activation 4 days later in PLNs (**E**). (**E**) CFSE profile and IFN-γ production of CD4$^+$Thy-1.1$^+$FoxP3$^-$ cells (left panels) and quantification of CD4$^+$Thy-1.1$^+$FoxP3$^-$IFNγ$^+$ cell numbers (right panel). In **A**–**D**, Teffs and Tregs were obtained from Thy-1.2 TCR-HA mice. Data were from 6 mice per group from 2 independent experiments. *$P < 0.05$; **$P < 0.001$. Error bars represent SD.

To further study the Teff→Treg boost using pure Treg population, we generated a high number of pure Tregs by in vitro Ag-specific stimulation using previously described conditions (32). Tregs expanded by a factor of 1,000 over a 4-week period and maintained potent suppressive activity in vitro (Supplemental Figure 1, A and B; supplemental material available online with this article; doi:10.1172/JCI42945DS1). As with freshly purified Tregs, a strong Teff→Treg boost was observed in ins-HA mice cotransferred with expanded HA-Tregs and activated HA-Teffs in PLNs (Figure 1, D and E). Expanded Tregs maintained high Foxp3 expression and the activation markers mentioned above as well as the CD103 Treg activation marker (20) and CD127, when they were cotransferred with Teffs (Supplemental Figure 1C). Interestingly, high numbers of divided islet-specific donor Tregs were also observed in the pancreas of mice cotransferred with expanded HA-Treg and preactivated HA-Teff in ins-HA mice (Supplemental Figure 2). When injected alone, we could hardly detect any HA-Tregs in the pancreas, probably due to their incapacity to migrate to this

tissue in the absence of inflammation. These findings showed that HA-specific transgenic Teffs led to a higher level of proliferation and expansion in PLNs and pancreas of HA-specific transgenic Tregs after adoptive transfer in ins-HA mice.

Paradoxical protective effect of diabetogenic Teffs in diabetes due to increased Treg activity. To explore the effect of the Teff→Treg boost in the physiopathology of autoimmune diseases, we first set up a model of diabetes in ins-HA mice. The transfer of preactivated HA-Teffs in these mice, but not of freshly purified cells, triggered a rapid autoimmune diabetes with hyperglycemia within 6 to 12 days (Figure 2A). The diabetogenic capacity of HA-Teffs was probably due to their strong reactivation in PLNs, as suggested by increased proliferation and IL-2 and IFN-γ production compared with freshly purified CD4$^+$ T cells (Supplemental Figure 3A). Ins-HA mice transferred with expanded HA-Tregs alone did not become diabetic. The cotransfer of expanded HA-Tregs prevented diabetes induced by activated HA-Teffs (Figure 2A). We then evaluated whether the Teff→Treg boost led to sustained dia-

Figure 3
Strong Teff→Treg boost in NOD mice. Four- to 7-week-old NOD mice were transferred with freshly purified CFSE-labeled CD45.2+ BDC2.5-Tregs alone or coinjected with pre-activated BDC2.5-Teffs. (**A**) Representative CFSE profile of donor Tregs (CD4+CD45.2+ cells gated as shown in the left panel) in pancreatic islets (islets), PLNs, and nondraining LNs (NdLN) 5 days after transfer. (**B**) Absolute number of divided donor Tregs (CFSE^{dim}CD4+CD45.2+FoxP3+ cells) in PLNs at day 5. Dots represent individual mice, and bars show the means pooled from 3 independent experiments. ***$P < 0.0001$.

betes protection by challenging the mice with activated HA-Teffs 3 weeks later. Most of the mice initially cotransferred with HA-Tregs and HA-Teffs did not develop diabetes after the challenge (Figure 2B). In contrast, mice initially transferred with HA-Tregs alone became diabetic 8 to 12 days after the challenge. Similar findings were obtained with freshly purified HA-Tregs (Supplemental Figure 3B). Since activated HA-Teffs, obtained after purification of CD25− cells and in vitro stimulation, contained both CD4+ and CD4− cells, we investigated which cell population was responsible for the sustained Treg-mediated regulation of diabetes. Only the CD4 fraction of the Teff population led to diabetes protection after challenge with the Teffs, presumably through increased expansion and activation of cotransferred Tregs (Figure 2C). Altogether, our results demonstrate that when Tregs were boosted by Teffs, mice were protected from diabetes induced by subsequent injection of activated Teff.

The protection from diabetes challenge conferred by the Teff→Treg boost could simply be explained by the increased number of donor Tregs compared with mice injected with Tregs alone. Additionally, the boost may also improve the intrinsic suppressive function of Tregs. Since mice that received HA-Tregs and activated HA-Teffs contained 10 times more donor Tregs in PLNs at the time of challenge (day 21) as mice that received HA-Tregs alone, we repeated the experiment by initial injection of either expanded HA-Tregs plus HA-Teffs or 10 times more Tregs alone. As expected, both groups of mice had similar numbers of HA-Tregs in PLNs at day 21 and even at a high number, HA-Tregs were not activated when transferred alone (Supplemental Figure 4). At this time, mice were challenged with activated HA-Teffs. Only mice that received HA-Tregs plus HA-Teffs were protected from the diabetes challenge (Figure 2D), suggesting that Teffs not only increased the proliferation/expansion of Tregs but also their suppressive activity. We confirmed this finding in an in vivo suppressive assay. Ins-HA mice were similarly injected with HA-Tregs plus HA-Teffs or 10 times more HA-Tregs alone or with PBS. Three weeks later, mice were challenged with activated HA-Teffs to assess their activation in PLNs at day 4. In PBS control mice, HA-Teffs strongly proliferated and secreted high amounts of IFN-γ in PLNs (Figure 2E). This activation was significantly reduced in mice that received previously high amounts of HA-Tregs alone. Interestingly, HA-Teff activation was further suppressed in mice that were initially cotransferred with low amounts of HA-Tregs and HA-Teffs (Figure 2E). These experiments showed that the Teff→Treg boost not only increased the number and activation of Tregs but also enhanced their suppressive function.

Islet-specific Teffs boost islet-specific and polyclonal Tregs in NOD mice. We then explored whether the Teff→Treg boost phenomenon was also observed in the spontaneous and more physiological diabetes model of NOD mice. Similar adoptive transfer experiments were performed, using islet-specific Teffs and Tregs purified from the BDC2.5 TCR transgenic mice (33). Young NOD mice were injected with freshly purified Tregs from BDC2.5 mice (BDC-Tregs) alone or coinjected with preactivated T cells from BDC2.5 mice (BDC-Teffs). After 5 days, BDC-Tregs injected alone weakly divided and accumulated in PLNs. The cotransfer of BDC-Teffs induced a strong increase in the proliferation and expansion of BDC-Tregs (Figure 3, A and B), as observed in the ins-HA model (Figure 1). Interestingly, Teffs of the nontransgenic BDC2.5 clone, derived from diabetic NOD mice (34), were also able to boost BDC-Tregs in PLNs (data not shown). Since pancreatic islets of NOD mice are spontaneously inflamed after 3 weeks of age, favoring migration of activated islet-specific T cells in the pancreas, we evaluated the presence or not of a Teff→Treg boost in this tissue. As for PLNs, the cotransfer of preactivated BDC-Teffs dramatically increased the proliferation of BDC-Tregs in the pancreas (Figure 3A). No division was observed in the nondraining LNs because of the absence of islet-antigen presentation.

In order to go one step further in assessing the physiological relevance and extent of the Teff→Treg boost phenomenon, we analyzed whether it was also observed on polyclonal endogenous Tregs. We thus determined whether the administration of activated BDC-Teffs in NOD mice induced an increase in the proliferation
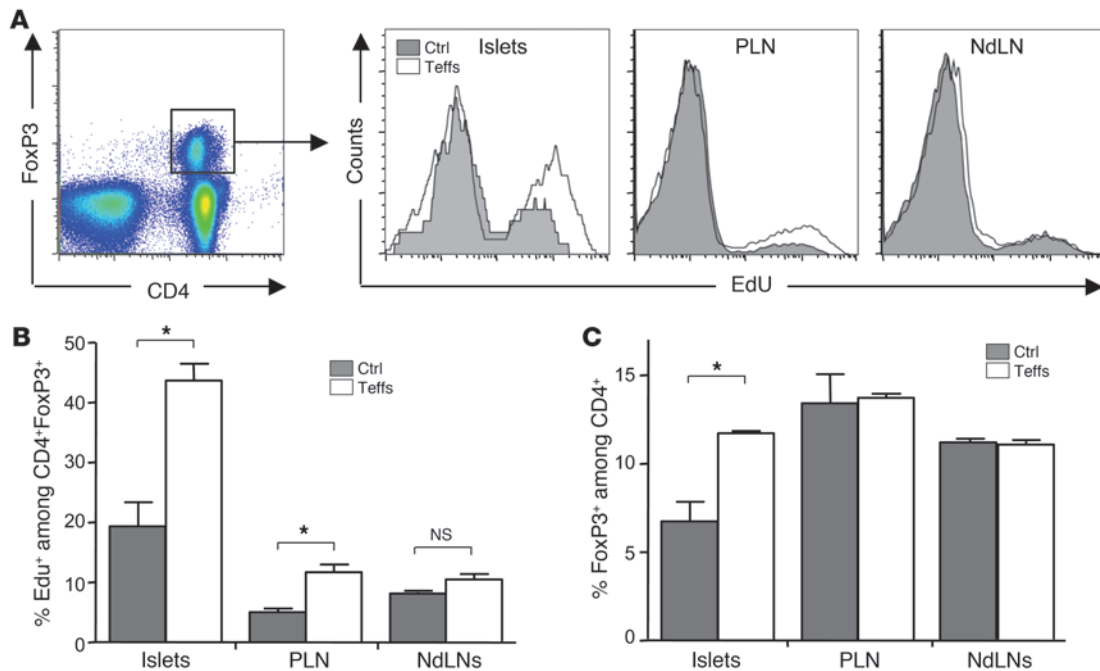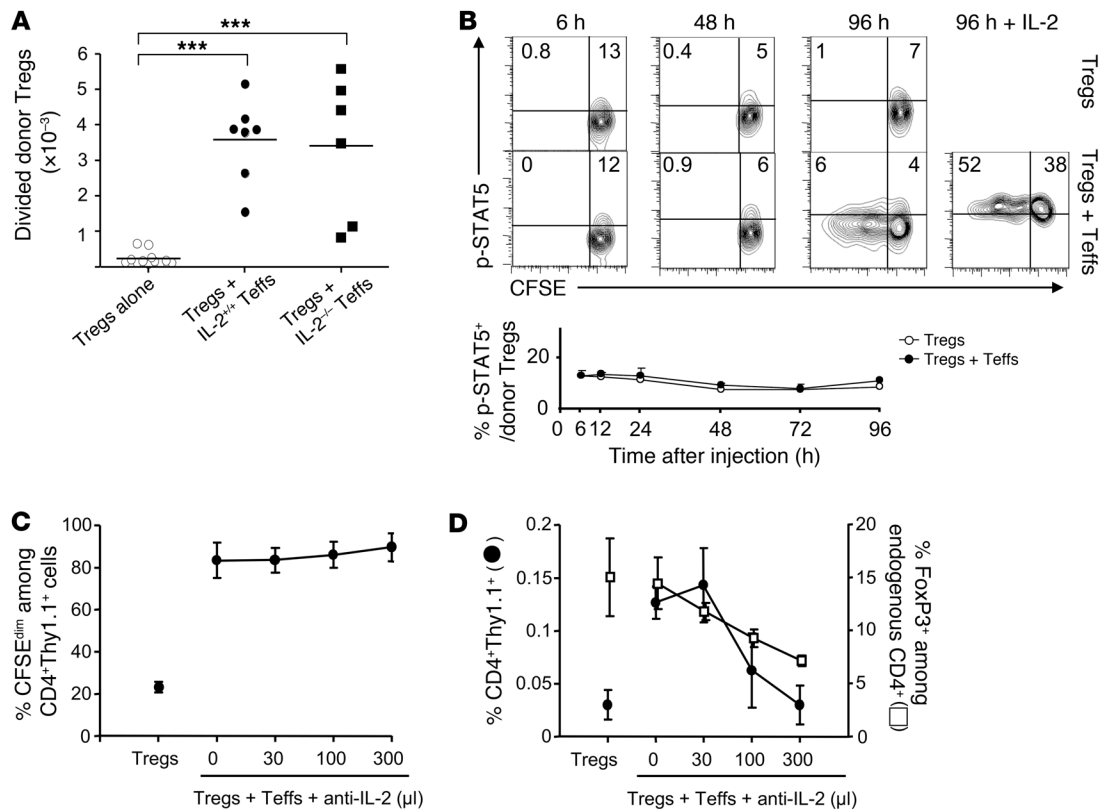
Figure 4
Islet-specific Teffs boost polyclonal endogenous Tregs. Four- to 7-week-old NOD mice were injected with PBS (Ctrl) or transferred with preactivated CD45.2+ BDC-Teffs. Mice were administered with the nucleotide analog EdU at days 2 to 4 and sacrificed at day 4 to analyze proliferation of endogenous Tregs. Representative profile (**A**) and mean from 1 representative out of 4 independent experiments (**B**) of DNA incorporation of EdU among endogenous Tregs (CD4+FoxP3+CD45.2−) in pancreatic islets, PLN, and NdLNs. (**C**) Fold increase of the percentage of endogenous FoxP3+ cells among CD4+ cells between BDC-Teff–injected mice and PBS-injected mice. Mean data were obtained from 1 representative out of 4 independent experiments. *P < 0.05. Error bars represent SD.

of endogenous Tregs. In control mice receiving PBS, we observed a low basal proliferation of endogenous Tregs in LNs and a higher one in pancreatic islets (Figure 4, A and B), as we had previously reported (29, 35). The administration of BDC-Teffs induced an increase in the proliferation of endogenous Tregs in the pancreas and PLNs but not in nondraining LNs (Figure 4, A and B). This led to an increase of the proportion of Tregs among CD4+ T cells only in the pancreas (Figure 4C). Altogether, these findings show that the Teff→Treg boost phenomenon is observed in different genetic backgrounds and with different T cell clones.

The Teff→Treg boost is not IL-2 dependent. We then started to explore the molecular mechanism involved in the Teff→Treg boost. IL-2 was an obvious candidate, since this cytokine is secreted shortly after T cell activation and is a potent Treg proliferation factor in vivo (36–39). We thus tested whether the Teff→Treg boost was mediated by IL-2 produced by Teffs using IL-2–deficient HA-Teffs from TCR-HA transgenic mice crossed to IL-2 KO mice. As shown in Figure 1, activation of transferred expanded HA-Tregs was strongly enhanced when IL-2–sufficient HA-Teffs were coinjected in ins-HA mice. Surprisingly, this strong Teff→Treg boost was still observed using IL-2–deficient HA-Teffs (Figure 5A). Similar findings were obtained with freshly purified HA-Tregs (Supplemental Figure 5). Thus, the Teff→Treg boost was not dependent on IL-2 produced by HA-Teffs. However, we could not rule out that IL-2–deficient activated Teffs would increase the levels of endogenous IL-2 produced by other cells, such as recipient Teffs or DCs. We thus analyzed by flow cytometry phosphorylation of STAT5 (p-STAT5) in Tregs, as a downstream marker of IL-2 signaling (39).

When analyzed at various time points for 4 days after cell transfer, only a small fraction of p-STAT5+ cells was detected within donor Tregs in mice that received Tregs alone. This proportion was not increased in mice that were cotransferred with Teffs (Figure 5B). As a control experiment, we checked that almost all Tregs became p-STAT5+ after administration of high-dose IL-2 3 hours before sacrifice at day 4 in mice receiving Teffs plus Tregs (Figure 5B). Furthermore, low- and high-dose IL-2 injected in control BALB/c mice resulted in enrichment of p-STAT5+ cells in Tregs that was detectable for at least 12 hours (Supplemental Figure 6). Thus, our results showed that no enrichment of p-STAT5 over basal levels was observed in Tregs at any time point during the Teff→Treg boost, suggesting that IL-2 was not involved. To further rule out a role of IL-2 in the Teff→Treg boost, we neutralized IL-2 with a mAb. The increased division of HA-Tregs induced by HA-Teffs was not reduced in the presence of increasing doses of anti–IL-2 mAb (Figure 5C). As expected (36), neutralizing IL-2 altered equally the survival of recipient and donor Tregs depending on the dose of anti–IL-2 mAb (Figure 5D). Altogether, these data showed that the increased Treg proliferation of boosted Tregs was not due to IL-2.

Tregs are boosted by Teffs in vitro and acquire a distinct RNA signature. To gain insight into the molecular mechanism of the Teff→Treg boost, we performed a microarray gene analysis to analyze the molecular pathway(s) modified in boosted Tregs. To gain access to enough cells for this kind of analysis, we first set up an in vitro model of the Teff→Treg boost that was not dependent on IL-2. HA-Tregs were cultivated for 5 days with HA-pulsed DCs alone or with freshly purified IL-2–sufficient or IL-2–deficient HA-Teffs in the
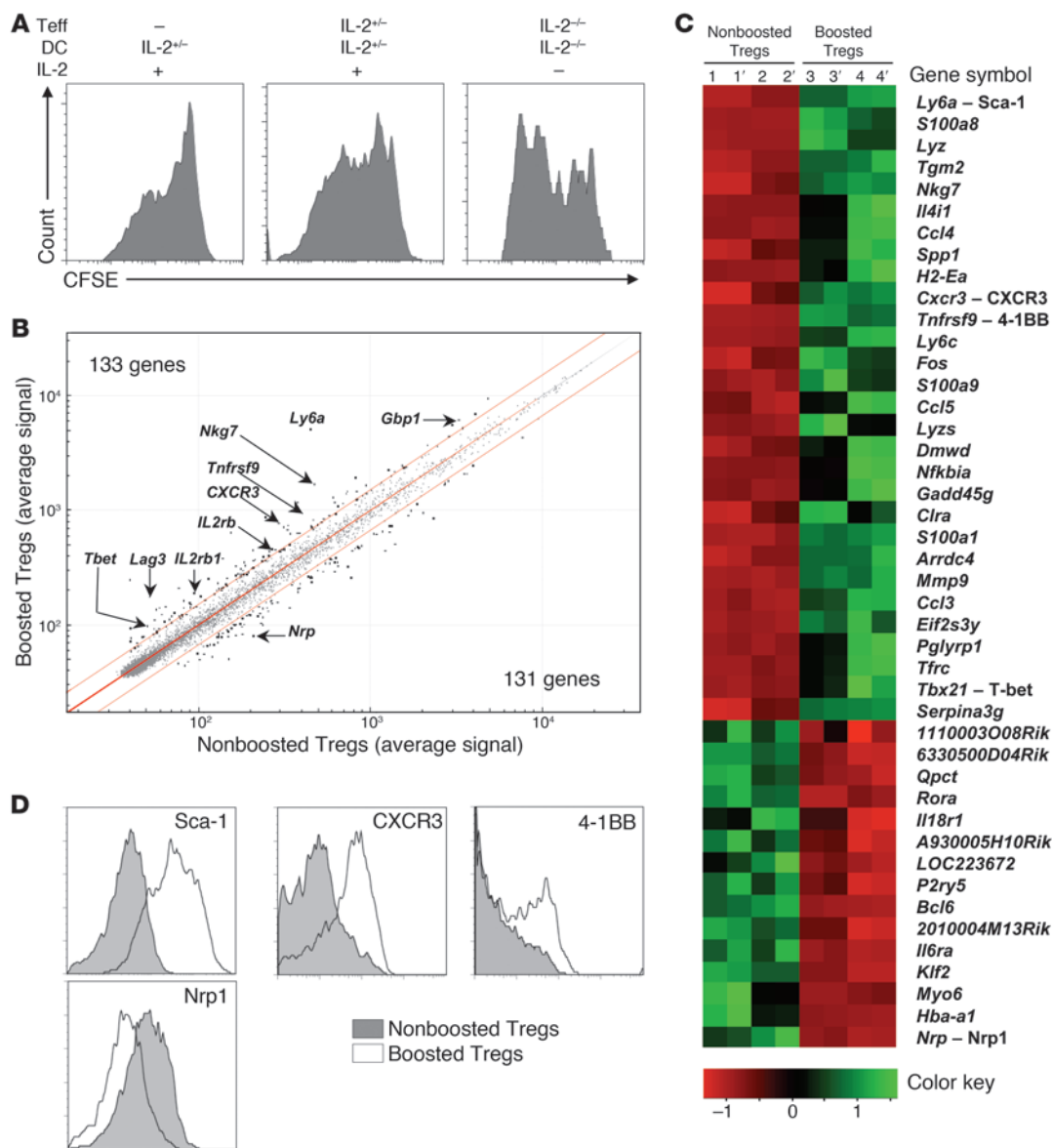
Figure 5

The Teff→Treg boost is not mediated by IL-2. (**A**) Ins-HA mice were transferred with CFSE-labeled Thy-1.1+ expanded HA-Tregs alone or coinjected with preactivated HA-Teffs from IL-2–deficient or IL-2–sufficient littermate control mice. Divided HA-Treg numbers (CFSE^{dim}CD4+Thy-1.1+ cells) were quantified in PLNs 10 days later. Dots represent individual mice, and bars show the means from at least 2 independent experiments. ***$P < 0.0001$. (**B**) Ins-HA mice were transferred with CFSE-labeled Thy-1.1+ expanded HA-Tregs alone or coinjected with IL-2–sufficient HA-Teffs. Phosphorylation of STAT5 on donor Tregs (CD4+Thy-1.1+FoxP3+) was determined at the indicated times in the PLN. Top panels show representative data from 2 independent experiments. Horizontal and vertical lines delineate positive p-STAT5 staining and undivided cells, respectively. At 96 hours, some mice were injected with 250,000 IU of human IL-2 3 hours before sacrifice as a positive control for phosphorylated STAT5 staining (right panel). The bottom graph represents the mean of 1 to 3 mice per time point from 2 independent experiments. (**C** and **D**) Ins-HA mice were transferred with CFSE-labeled Thy-1.1+ expanded HA-Tregs alone or coinjected with preactivated HA-Teffs. Various doses of anti–IL-2 mAb (S4B6 mAb, expressed in μl of ascites) were administered to block IL-2 after cell transfer. 10 days later, percentage of divided cells among donor Tregs (**C**) as well as percentages of whole donor Tregs (black circles) and endogenous Tregs (white squares) (**D**) were quantified in PLNs. Representative data of 2 independent experiments with 2 or 3 mice per group. Error bars represent SD.

presence or not of exogenous IL-2. As expected, Tregs stimulated by DCs in the presence of IL-2 proliferated in vitro (Figure 6A). Importantly, this proliferation was increased when IL-2–sufficient HA-Teffs were added to the culture. Surprisingly, proliferation of Tregs cultivated with IL-2–deficient Teffs and DCs in the absence of exogenous IL-2 was even more important (Figure 6A), despite an expected loss of Treg survival (36) (data not shown). This data showed the existence of an IL-2–independent Teff→Treg boost in vitro, allowing us to use this model to compare the transcriptome of nonboosted and boosted Tregs. HA-Tregs were cultured with or without HA-Teffs for 5 days in the presence of exogenous IL-2 to maintain their survival and then sorted using a congenic marker to analyze their transcriptome by gene array. Boosted Tregs exhibited a specific RNA signature. Using a 1.5-differential fold-change expression cut-off, 133 genes were upregulated and 121 were downregulated in boosted Tregs compared with nonboosted Tregs. Among the upregulated genes, several belong to the so-called "Treg signature" (40), such as *Ly6a*, *Nkg7*, *Lag3*, *Tnfrsf9*

(4-1BB), *Gbp1*, *IL2rb*, and *Pdcd1lg1* (PD-L1) (Figure 6B). The list of genes with a 2-differential fold-change expression cut-off is shown in heat-map data (Figure 6C). We confirmed by flow cytometry that boosted Tregs upregulated Ly-6A (Sca-1), CXCR3, and 4-1BB and downregulated neuropilin-1 (Nrp1) (Figure 6D). The modulation of Sca-1 and Nrp1 expression in boosted Tregs was also confirmed in vivo (Supplemental Figure 7).

To have a more synthetic view of the molecular pathways modified in boosted Tregs, the data were processed through the Ingenuity pathway analysis software. Interestingly, the expression of the molecules of the alternative NF-κB pathway (NIK/IKKα/p52/RelB) was upregulated in boosted Tregs (Supplemental Figure 8). This suggested that member(s) of the TNFR super-family that signal through this pathway, such as lymphotoxin-βR or TNF receptor 2 (TNFR2) (41), could be involved in the Teff→Treg boost. TNF became a potential candidate because (a) this cytokine is produced by activated Teffs, (b) its interaction with TNFR2 expressed by activated Tregs promote their expansion (42), and (c) boosted Tregs expressed TNFR2 (data
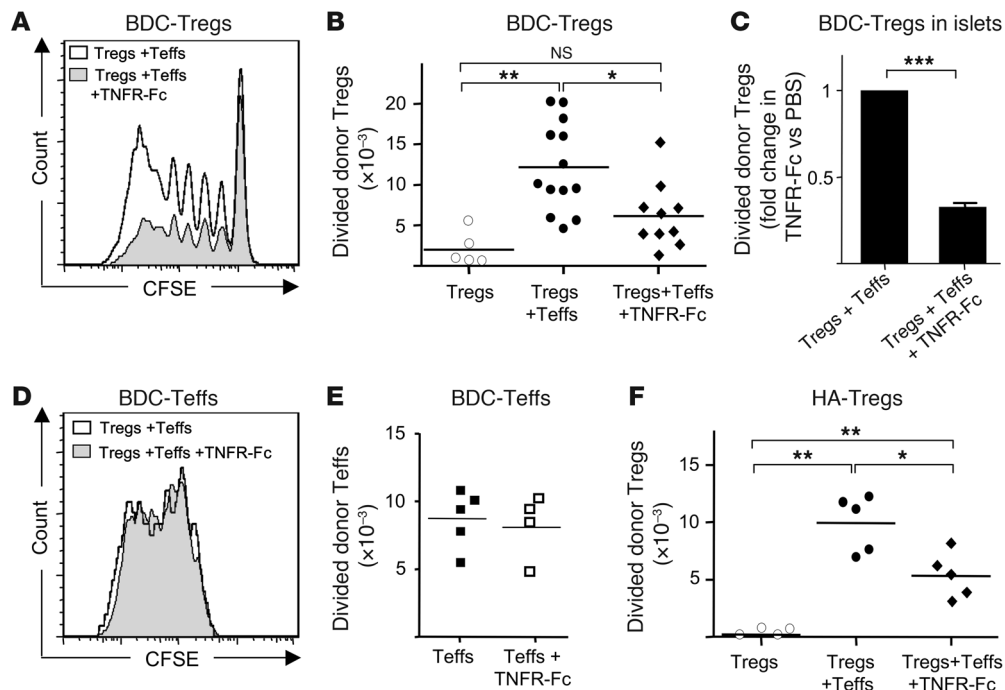
Figure 6
Tregs boosted in vitro by Teffs change their phenotype. (**A**) Expanded CFSE-labeled Thy-1.1+ HA-Tregs were cultured for 5 supplemental days with IL–2–sufficient or –deficient HA-pulsed DCs alone or with freshly-purified IL-2–sufficient or –deficient HA-Teffs, in the presence or not of IL-2. Representative CFSE profile of CD4+Thy-1.1+ Tregs out of 3 independent experiments. (**B** and **C**) Comparison of the transcriptome of expanded HA-Tregs after 5 days of culture with IL-2, HA-pulsed DCs in the presence (boosted Tregs) or absence (nonboosted Tregs) of IL-2–sufficient Teffs. (**B**) Scatter plot comparison of average expression values in boosted Treg versus nonboosted Treg for all the 45,282 probes. Threshold lines were drawn at 1.5–fold-change expression (*P* ≤ 0.05), and significant probes were depicted as bold spots. Genes of interest are indicated by their symbol names. (**C**) Heat map of distinct expression profiles revealed by microarray analysis of the nonboosted (biological samples 1 and 2) and boosted Treg populations (samples 3 and 4). Apostrophes indicate technical replicates of each biological sample. The genes were selected based on a fold-change ≥ 2 (*P* ≤ 0.05). A color code scale indicates fold-change variation. (**D**) Tregs were cultured for 5 days as in **B**. Expression of the indicated molecules was compared when Tregs were cultivated with or without HA-Teffs. Histograms are representative of 2 independent experiments.

not shown). We thus tested the role of TNF in the Teff→Treg boost in NOD mice. Strikingly, when we blocked TNF using a TNFR2-Fc soluble receptor antagonist (blocking both TNF-α and TNF-β, also known as lymphotoxin-α), the Teff→Treg boost was significantly reduced, although not fully abolished in PLNs (Figure 7, A and B) and the pancreas (Figure 7C). Administration of a blocking mAb that neutralized only TNF-α similarly diminished the Treg boost

(Supplemental Figure 9). An important control was to check that the reduced Teff→Treg boost observed when TNF was neutralized was not due to a decreased Teff activation. This was not the case, since proliferation and expansion of Teffs were not reduced when blocking TNF (Figure 7, D and E). Similar findings were obtained in ins-HA mice (Figure 7F). These findings showed that part of the Teff→Treg boost was mediated by TNF-α.

Figure 7

The Teff→Treg boost is TNF dependent. (**A–C**) Four- to 6-week-old NOD mice were transferred with freshly isolated CFSE-labeled CD45.2[+] BDC2.5-Tregs alone or coinjected with preactivated CD45.1^{+} BDC2.5-Teffs with or without TNFR2-Fc treatment. Representative CFSE profile (**A**) and absolute number of divided donor Tregs (CFSE^{dim}CD4^{+}CD45.2^{+}FoxP3^{+} cells) in PLNs 5 days after transfer (**B**) from 6 independent experiments. Each symbol represents an individual mouse and bars show the means. (**C**) Relative accumulation of divided donor Tregs in the pancreas of TNFR2-Fc–treated mice compared with PBS-treated mice 5 days after transfer. Data are from 5 independent experiments with 6 mice per group. (**D** and **E**) Representative CFSE profile (**D**) and absolute number (**E**) of donor Teffs (CD4^{+}CD45.2^{+}FoxP3^{−} cells) in PLNs 5 days after cotransfer of CD45.2^{+} Teffs and CD45.1^{+} Tregs in mice treated with saline or TNFR-Fc. (**F**) Ins-HA mice were injected with CFSE-labeled Thy-1.1^{+} expanded HA-Tregs alone or with preactivated HA-Teffs with or without TNFR-Fc treatment. Absolute numbers of divided donor Tregs (CFSE^{dim}CD4^{+}Thy-1.1^{+} cells) were quantified in PLNs at day 7 after cell transfer. Each symbol represents an individual mouse, and bars show the means pooled from 3 independent experiments. $*P < 0.05$; $**P < 0.001$. Error bars represent SD.

Discussion

In this study, we show that activated Teffs boost the expansion and suppressive function of Tregs in vivo by a TNF-dependent mechanism. The Teff→Treg boost may be important to prevent or limit autoimmunity when a tissue or organ is inflamed. We observed that preactivated diabetogenic Teffs are more efficient than freshly purified nondiabetogenic Teffs in boosting Treg activity. Consequently, Treg-mediated suppression is strengthened when most needed, i.e., under the condition of strong activation of autoreactive Teffs and subsequent risk of autoimmunity. Linking Treg expansion to Teff activation would generate a feedback regulatory loop for dynamically tuning the size of Treg populations to their target Teffs locally. Our data also raise the intriguing conclusion that the very same cells that have the capacity to induce diabetes can also favor disease protection when cotransferred with islet-specific Tregs. In the ins-HA model, the cotransfer of Tregs prevented diabetes induced by Teffs. The protective function of Tregs may be enhanced by the Teff→Treg boost, since it was detectable as soon as day 4, before diabetes onset in mice injected with Teffs only. In mice that received islet-specific Teffs and Tregs, we believe that diabetes protection at 3 weeks from a new challenge with Teffs was due to the presence of an increased number of highly suppressive donor Tregs. However, we cannot formally exclude that disease protection was acquired because of the establishment of a

local tolerogenic environment or because transferred Teffs became themselves tolerogenic, even if they did not acquire FoxP3 expression (data not shown). Thus, in autoimmune diseases, Teffs should be considered as either pathogenic or protective, as a result of the 2-way interaction between Tregs and Teffs.

The balance between activated Teffs and activated Tregs is critical for maintaining a healthy immune status. Persistent activation of Teffs, uncontrolled by Tregs, would lead to chronic inflammation and possibly autoimmune diseases. Conversely, too strong Treg-mediated suppression could lead to poor antiinfectious and antitumor immune responses. In biology, stable homeostatic balance usually depends on feedback mechanisms. Our data show that Teff activation increases proliferation of Tregs and their suppressive function. This feedback mechanism would favor the maintenance of Teff/Treg equilibrium, as shown in a proposed model (Supplemental Figure 10). In an inflammatory state with strong and sustained Teff activation, Teffs promote factors favoring a Treg boost, leading to subsequent Treg expansion. This expansion strengthens Treg-mediated suppression acting on Teffs, possibly perpetuating a dynamic Teff/Treg equilibrium and a state of localized and stable chronic inflammation, as described in some infectious diseases (43). Alternatively, the strong inhibition of Teff activation by boosted Tregs may lead to a decrease of factors promoting the Teff→Treg boost, leading to weak Treg-mediated sup-

pression, favoring a return to basal homeostatic Teff/Treg equilibrium. In a simplified view, Teff/Treg equilibrium may result from the fact that Tregs inhibit Teff activity whereas Teffs promote Treg activity, reminiscent of feedback mechanisms observed in homeostatic regulation of hormone secretion (e.g., hormones of the hypothalamic-pituitary-adrenal axis glands). A defect of the Teff→Treg boost may be one factor, among others, that coalesce for the establishment of an autoimmune disease.

This theoretical dynamic interaction between Tregs and Teffs inferred from our data and schematized in Supplemental Figure 10 may explain the relapsing/remitting status of several autoimmune diseases. During EAE, an animal model of multiple sclerosis, Teffs first colonize the central nervous system, where they extensively proliferate during the acute phase of the disease. This is followed by a secondary active Treg proliferation and then disease remission, due to the presence of Tregs (17, 44, 45). One may envisage that the primary Teff activation promotes a Teff→Treg boost, favoring remission. Then, because of the low level of Teff activation during remission, the Teff→Treg boost is weakened, leading to lower Treg suppressive activity, opening a window for disease relapse when a new wave of Teffs colonizes the target tissue.

What are the factors involved in the Teff→Treg boost phenomenon? IL-2 was an obvious candidate. Previous studies showed that a low level of IL-2, presumably produced by $CD25^{lo}$ Teffs, is critical for the survival and homeostasis of Tregs. This effect may serve to maintain a physiological and stable equilibrium between Teffs and Tregs at the steady state (36, 46, 47). During an immune response, IL-2 produced by activated Teffs has also been reported to increase Treg expansion (39). In the Teff→Treg boost described here, IL-2 was necessary to maintain Treg survival and was thus critical to preserving a high number of boosted Tregs, but was clearly not involved in the increased Treg proliferation mediated by Teffs. In this line, we recently observed that administration of low-dose IL-2 induced diabetes prevention in NOD mice. This effect was associated with an increased Treg proportion in the pancreas, not due to an increase of their division, but probably to a better survival (35, 48). Also, administration of low-dose IL-2 in ins-HA mice that received HA-Tregs alone did not increase their proliferation in PLN at day 8 (data not shown). Furthermore, an increased expression of CD127 was observed on boosted Tregs, suggesting that IL-7 may be also involved in Treg survival, as previously observed in another context (49). TNF-α was clearly involved, since blocking this cytokine significantly reduced the Teff→Treg boost without inhibiting Teff activation. Interestingly, after TNF-α blockade, the fewer divided Tregs still went through an equal amount of divisions. This suggests that this cytokine is involved either in the entry into cycling of Tregs or in the viability of dividing Tregs. Future experiments will be required to determine what cellular source or sources of TNF-α are critical for the boost. In this line, TNF-α production was detected on Teffs, Tregs, and antigen-presenting cells in mice receiving Teffs and Tregs (data not shown). Our data are compatible with a previous report showing that interaction of TNF-α with TNFR2, but not TNFR1, promoted expansion of Tregs in vitro (42). Blocking TNF-α did not fully inhibit the Teff→Treg boost, suggesting that other molecular pathways are involved.

Further study of the transcriptome data comparing boosted versus nonboosted Tregs may provide indications on other molecule or molecules involved in the Teff→Treg boost. The following canonical pathways were preferentially modified in boosted Tregs: energy and cell cycling metabolism, costimulation (CD28, CD40, CD27, and 4-1BB), cytokine (IL-6, IL-2, IL-12 and lymphotoxin-βR), chemokine (IL-8, CCR5, CXCR4 and CXCR3), glucocorticoid receptor, aryl hydrocarbon receptor, and NF-κB (Supplemental Table 1), revealing a complex and multifactorial phenomenon associated with the Teff→Treg boost. 4-1BB or ICOS may play a role because of their increased expression in boosted Tregs and their described capacity to favor Treg proliferation (50, 51). IFN-γ may be also involved since boosted Tregs expressed increased level of CXCR3 and T-bet, both upregulated by IFN-γ signaling, and T-bet–positive Tregs have increased proliferative response (31). Overall, our phenotypic, functional, and transcriptome analyses indicate that boosted Tregs acquire new properties with major gene expression modifications, an activated phenotype, and increased suppressive capacity.

Our findings may help explain intriguing and unresolved observations on the role of TNF-α in certain autoimmune diseases. Contrary to expectation, because of the well-established proinflammatory property of this cytokine, mice deficient in TNF-α (KO or treated with neutralizing antibody) developed more severe lupus, EAE, and diabetes, whereas TNF-α administration has therapeutic effects in these diseases (52–54). Also, TNF-α neutralization in patients with multiple sclerosis exacerbated the disease (55). The immunoregulatory role of TNF-α may be explained by its capacity to boost Treg activity. Indeed, spontaneous disease remission observed in EAE, which follows high Treg expansion (44), is abolished either by depleting Tregs (45) or in TNF-α–deficient mice (52, 53). Furthermore, TNF-α seems to exert its regulatory role by signaling through TNFR2 rather than TNFR1 since EAE was exacerbated in TNFR2-KO mice and reduced in TNFR1-KO mice (56). Again, this is compatible with a role of TNF-α acting on Tregs, since the interaction of this cytokine with TNFR2, and not TNFR1, promotes Treg expansion (42). We thus propose that during EAE, activated pathogenic Teffs promote TNF-α production, which induces a Teff→Treg boost via TNF/TNFR2 interaction, leading to disease remission. Our work reveals a new feedback mechanism that may have an essential role in slowdown or reduce certain immunopathologies.

Molecules able to boost Treg activity are under extensive investigation for their therapeutic potential in immunopathologies. IL-2 is being investigated in the treatment of autoimmune diseases (57). For instance, we recently showed that administration of low-dose IL-2 induced diabetes remission in new-onset diabetic NOD mice, probably by increasing Treg survival and function in the pancreas (35, 48). The Teff→Treg boost described in this work may lead to identifying other therapeutic molecules, such as TNF-α. Combining molecules promoting survival (such as IL-2) and proliferation (such as TNF-α) of Tregs may have a therapeutic interest. Further studies are required to define their proper utilization.

Methods

Mice. Six- to 8-week-old BALB/cByJ (BALB/c) mice were obtained from Charles River Laboratories. Ins-HA transgenic mice expressing HA under the control of the insulin promoter were backcrossed more than 10 generations onto a BALB/c genetic background (29). The TCR-HA transgenic mice that express a transgenic TCR recognizing the HA_{111} epitope presented by $I-E^d$ (58) were backcrossed more than 10 generations onto a BALB/c genetic background. Some of these mice were bred with Thy-1.1 BALB/c congenic mice and with IL-2–KO BALB/c mice. BDC2.5-TCR transgenic mice (33) and NOD-CD45.2 congenic mice were backcrossed more than 10 generations onto a NOD genetic background. All of these mice were bred in our animal facility under specific pathogen–free conditions. Harald von Boehmer, Nicolas Glaichenhaus, and Kathryn Haskins provided TCR-HA transgenic

mice, WT15 LACK-specific TCR transgenic mice, and the BDC2.5 clone, respectively. Manipulations were performed according to European Economic Community guidelines and under approval of the Regional Ethics Committee in Animal Experiment N°3 of Ile-de-France region.

Cell preparation and adoptive transfer. Cells were prepared as previously described (29). Briefly, LNs (brachial, axillary, cervical, and inguinal) and spleen were mechanically dissociated. Cells, incubated with biotin-labeled anti-CD25 mAb (7D4; BD Biosciences), were coated with anti-biotin microbeads (Miltenyi Biotec). The CD25$^+$ cell fraction (Tregs) was obtained after 2 consecutive runs on magnetic cell separation LS columns (Miltenyi Biotec), reaching 85% purity of CD25$^+$ cells. The CD25$^-$ cells were harvested from the flow through. This fraction contained 30% CD4$^+$ T cells and 0.5% residual CD25$^+$ cells.

To obtain in vitro–expanded HA-Tregs, we started the culture with 99% pure CD62L^{hi}CD4$^+$CD25^{hi} cells, purified by flow cytometry from the CD25$^+$ cell fraction of TCR-HA mice. Then cells were stimulated every week with splenic DCs purified using anti-CD11c–coupled beads (Miltenyi Biotec) presenting the HA peptide for 3 to 4 weeks as previously described (32). To obtain preactivated Teffs, the CD25$^-$ fractions from TCR-HA or TCR-BDC2.5 mice were stimulated in vitro for 3–4 days by HA peptide–pulsed (10 μg/ml; Neosystems) splenic DCs or by irradiated NOD splenocytes, pulsed with 2 μg/ml of the p31 peptide (BDC antigenic mimotope, amino acids sequence YVRPLWVRME; Neosystems) in the presence of 10 ng/ml of GM-CSF. Before intravenous injection, cells were labeled with 2.5 μM CFSE for 5 minutes in PBS at room temperature and were washed twice in PBS. When freshly purified Tregs were used, mice received 1 × 10^6 Tregs with or without 1 × 10^6 CD25$^-$ cells. When expanded Tregs were used, mice received 2 × 10^6 Tregs with or without 2 × 10^6 CD25$^-$ cells.

Antibodies and flow cytometry analysis. The following mAbs from BD Biosciences, e-Bioscience, and BioLegend were used: allophycocyanin-labeled (APC-labeled), PerCP-labeled or Alexa Fluor 700–labeled anti-CD4; PE- or PerCP-labeled anti–Thy-1.1; PE-labeled anti-CD45.2; APC-labeled anti-CD25; APC-labeled anti-ICOS; APC-labeled anti-GITR; APC-labeled CD44; PE-labeled anti-CTLA-4; biotinylated anti-TNFR2; PE-labeled anti-Sca-1; biotinylated anti-CXCR3;, biotinylated anti–4-1BB; purified goat anti-mouse anti-Nrp-1 (R&D Systems) followed by swine and goat-PE (Caltag); and PE-labeled anti–IFN-γ and anti–IL-2. Biotinylated antibodies were revealed by Percp or APC streptavidins. The unlabeled 6.5 Ab was revealed by a biotin-labeled anti-rat IgG2b (SouthernBiotech) followed by streptavidin-APC (BD Biosciences) staining. The PE- or Pacific blue–labeled anti-Foxp3 staining was performed using the eBioscience kit and protocol. 5-ethynyl-2′-deoxyuridine (EdU) incorporation was measured by using the Click-iT EdU Flow Cytometry Assay Kit (Molecular Probes) after FoxP3 staining. For intracellular cytokine staining, cells were restimulated by HA-pulsed splenocytes for 6 hours (Supplemental Figure 3) or with PMA (Sigma-Aldrich) and ionomycin (Sigma-Aldrich) for 4 hours (Figure 2E) in the presence of Golgi-Plug (BD Biosciences). After cell surface staining, intracellular staining was performed using the CytoFix/CytoPerm kit and protocol (BD Biosciences). For phospho-STAT5 staining, LNs were dilacerated and immediately fixed in PBS with 1.5% formaldehyde for 10 minutes. After washing and 10 minutes permeabilization in MeOH previously chilled at 4°C, cells were washed twice and stained in PBS with 0.2% BSA and 0.09% NaN3 medium containing a cocktail of anti-CD4, anti-CD8, anti-CD25, anti-Thy1.1, anti-Foxp3, and anti–p-STAT5 mAbs. In control stainings using an inhibitory peptide that blocks specifically the binding of anti–p-STAT5 mAb to its target (a gift from R. Balderas; BD), we did not detect any p-STAT5$^+$ cells among Tregs. Cells were acquired on a FACSCalibur or an LSR II (BD Biosciences) and analyzed with CellQuest (BD Biosciences) or FlowJo (Tree Star) software.

Proliferation monitoring by EdU incorporation. To assess endogenous cell division, NOD mice injected with PBS or 3 million activated CD25$^-$ cells

received 4 i.p. injections every 12 hours of 1 mg of EdU (Molecular Probes), a nucleoside analog of thymidine that incorporates into dividing DNA, and were sacrificed 4 hours after the last EdU injection.

In vivo blockade of IL-2 and TNF. For IL-2 blockade, mice were administered with different volumes of the neutralizing anti–IL-2 mAb (S4B6) purified from ascites and injected at the same time as cell transfer. For TNF blockade, mice were administered with 1 mg of soluble TNFR2 (etanercept [Enbrel]; Wyeth) at days 0, 2, and 4 or with 0.5 mg of an anti–TNF-α mAb (XT3.11; BioXCell) at days 0, 2, and 4.

Diabetes induction. From 1 to 2 × 10^6 in vitro preactivated HA-Teffs, obtained as described above, were injected i.v. with or without equal numbers of Tregs into ins-HA transgenic mice. Blood glucose levels were monitored using a glucometer (OneTouch Basic, LifeScan Inc.) and were considered diabetic after 2 consecutive measurements over 250 mg/dl.

Sample generation and DNA microarray hybridization and analysis. Expanded HA-specific Thy-1.1 Tregs were cultured in the presence of murine IL-2 (10 ng/ml) with or without HA-specific Teffs. HA-pulsed DCs were put in 6-well plates with Tregs with or without Teffs in a ratio of 1 DC/5 Tregs/5 Teffs. After 5 days, CD4$^+$Thy-1.1$^+$ Tregs were sorted by flow cytometry. RNA was generated using RNeasy Mini kit (QIAGEN) and its quality was verified in an Agilent Bioanalyzer. Total RNA was amplified and converted to biotinylated cRNA according to the manufacturer's protocol (Illumina TotalPrep RNA Amplification Kit; Ambion). Two biological duplicates were hybridized to the Sentrix BeadChips Array mouse WG-6 v2 (Illumina) and read at the Pitie-Salpetriere P3S platform, Paris, France. Data extraction and normalization were performed using Quantile normalization in the BeadStudio software. The list of genes differently expressed in the boosted Tregs was used for pathway analysis. GenBank accession numbers (ArrayExpress E-MTAB-146) were imported into and mapped to the Ingenuity database using Ingenuity pathway analysis software (http://www.ingenuity.com) to model relationships among genes and proteins and to construct putative pathways and relevant biological processes.

Statistics. Statistical data were calculated using the 2-tailed unpaired Student t test. $P < 0.05$ was considered significant. For all the graphs, error bars represent SD.

Address correspondence to: Benoît L. Salomon or Eliane Piaggio, UPMC CNRS UMR7211 INSERM U959, Hôpital Pitié-Salpêtrière, 83 Bd de l'Hôpital, 75013 Paris, France. Phone: 33.1.42.17.74.66; Fax: 33.1.42.17.74.41; E-mail: benoit.salomon@upmc.fr (B.L. Salomon); elianepiaggio@yahoo.com (E. Piaggio).

1. Danke NA, Koelle DM, Yee C, Beheray S, Kwok WW. Autoreactive T cells in healthy individuals. *J Immunol*. 2004;172(10):5967–5972.

2. Horwitz MS, Bradley LM, Harbertson J, Krahl T, Lee J, Sarvetnick N. Diabetes induced by Coxsackie virus: initiation by bystander damage and not molecular mimicry. *Nat Med*. 1998;4(7):781–785.

3. Christen U, von Herrath MG. Initiation of autoimmunity. *Curr Opin Immunol*. 2004;16(6):759–767.

4. Gabrysova L, et al. Negative feedback control of the autoimmune response through antigen-induced differentiation of IL-10-secreting Th1 cells. *J Exp Med*. 2009;206(8):1755–1767.

5. Cuffy MC, et al. Induction of indoleamine 2,3-dioxygenase in vascular smooth muscle cells by interferon-gamma contributes to medial immunoprivilege. *J Immunol*. 2007;179(8):5246–5254.

6. Zhu C, et al. The Tim-3 ligand galectin-9 negatively regulates T helper type 1 immunity. *Nat Immunol*. 2005;6(12):1245–1252.

7. Salomon B, et al. B7/CD28 costimulation is essential for the homeostasis of the CD4+CD25+ immunoregulatory T cells that control autoimmune diabetes. *Immunity*. 2000;12(4):431–440.

8. Kim JM, Rasmussen JP, Rudensky AY. Regulatory T cells prevent catastrophic autoimmunity throughout the lifespan of mice. *Nat Immunol*. 2007;8(2):191–197.

9. Lahl K, et al. Selective depletion of Foxp3+ regulatory T cells induces a scurfy-like disease. *J Exp Med*. 2007;204(1):57–63.

10. Lund JM, Hsing L, Pham TT, Rudensky AY. Coordination of early protective immunity to viral infection by regulatory T cells. *Science*. 2008; 320(5880):1220–1224.

11. Shevach EM. Mechanisms of foxp3+ T regulatory cell-mediated suppression. *Immunity*. 2009; 30(5):636–645.

12. Wing K, Sakaguchi S. Regulatory T cells exert checks and balances on self tolerance and autoimmunity. *Nat Immunol*. 2010;11(1):7–13.

13. Curiel TJ, et al. Specific recruitment of regulatory T cells in ovarian carcinoma fosters immune privilege and predicts reduced survival. *Nat Med*. 2004;10(9):942–949.

14. Cao D, van Vollenhoven R, Klareskog L, Trollmo C, Malmstrom V. CD25brightCD4+ regulatory T cells are enriched in inflamed joints of patients with chronic rheumatic disease. *Arthritis Res Ther*. 2004;6(4):R335–R346.

15. Miyara M, et al. The immune paradox of sarcoidosis and regulatory T cells. *J Exp Med*. 2006; 203(2):359–370.

16. Uhlig HH, et al. Characterization of Foxp3+CD4+ CD25+ and IL-10-secreting CD4+CD25+ T cells during cure of colitis. *J Immunol*. 2006;177(9):5852–5860.

17. Korn T, et al. Myelin-specific regulatory T cells accumulate in the CNS but fail to control autoimmune inflammation. *Nat Med*. 2007;13(4):423–431.

18. McLachlan JB, Catron DM, Moon JJ, Jenkins MK. Dendritic cell antigen presentation drives simultaneous cytokine production by effector and regulatory T cells in inflamed skin. *Immunity*. 2009; 30(2):277–288.

19. Belkaid Y, Tarbell K. Regulatory T cells in the control of host-microorganism interactions (*). *Annu Rev Immunol*. 2009;27:551–589.

20. Huehn J, et al. Developmental stage, phenotype, and migration distinguish naive- and effector/memory-like CD4+ regulatory T cells. *J Exp Med*. 2004; 199(3):303–313.

21. Yamazaki S, et al. Direct expansion of functional CD25+ CD4+ regulatory T cells by antigen-processing dendritic cells. *J Exp Med*. 2003;198(2):235–247.

22. Fehervari Z, Sakaguchi S. Control of Foxp3+ CD25+ CD4+ regulatory cell activation and function by dendritic cells. *Int Immunol*. 2004;16(12):1769–1780.

23. Darrasse-Jeze G, et al. Feedback control of regulatory T cell homeostasis by dendritic cells in vivo. *J Exp Med*. 2009;206(9):1853–1862.

24. Takahashi T, et al. Immunologic self-tolerance maintained by CD25+CD4+ naturally anergic and suppressive T cells: induction of autoimmune disease by breaking their anergic/suppressive state. *Int Immunol*. 1998;10(12):1969–1980.

25. Thornton AM, Shevach EM. Suppressor effector function of CD4+CD25+ immunoregulatory T cells is antigen nonspecific. *J Immunol*. 2000; 164(1):183–190.

26. Billiard F, et al. Regulatory and effector T cell activation levels are prime determinants of in vivo immune regulation. *J Immunol*. 2006;177(4):2167–2174.

27. Klein L, Khazaie K, von Boehmer H. In vivo dynamics of antigen-specific regulatory T cells not predicted from behavior in vitro. *Proc Natl Acad Sci U S A*. 2003;100(15):8886–8891.

28. Walker LS, Chodos A, Eggena M, Dooms H, Abbas AK. Antigen-dependent proliferation of CD4+ CD25+ regulatory T cells in vivo. *J Exp Med*. 2003; 198(2):249–258.

29. Fisson S, et al. Continuous activation of autoreactive CD4+ CD25+ regulatory T cells in the steady state. *J Exp Med*. 2003;198(5):737–746.

30. Morgan DJ, Kreuwel HT, Sherman LA. Antigen concentration and precursor frequency determine the rate of CD8+ T cell tolerance to peripherally expressed antigens. *J Immunol*. 1999;163(2):723–727.

31. Koch MA, Tucker-Heard G, Perdue NR, Killebrew JR, Urdahl KB, Campbell DJ. The transcription factor T-bet controls regulatory T cell homeostasis and function during type 1 inflammation. *Nat Immunol*. 2009;10(6):595–602.

32. Fisson S, et al. Therapeutic potential of self-antigen-specific CD4+ CD25+ regulatory T cells selected in vitro from a polyclonal repertoire. *Eur J Immunol*. 2006;36(4):817–827.

33. Katz JD, Wang B, Haskins K, Benoist C, Mathis D. Following a diabetogenic T cell from genesis through pathogenesis. *Cell*. 1993;74(6):1089–1100.

34. Haskins K, Portas M, Bergman B, Lafferty K, Bradley B. Pancreatic islet-specific T-cell clones from nonobese diabetic mice. *Proc Natl Acad Sci U S A*. 1989;86(20):8000–8004.

35. Tang Q, et al. Central role of defective interleukin-2 production in the triggering of islet autoimmune destruction. *Immunity*. 2008;28(5):687–697.

36. Setoguchi R, Hori S, Takahashi T, Sakaguchi S. Homeostatic maintenance of natural Foxp3(+) CD25(+) CD4(+) regulatory T cells by interleukin (IL)-2 and induction of autoimmune disease by IL-2 neutralization. *J Exp Med*. 2005;201(5):723–735.

37. Zhang H, et al. Lymphopenia and interleukin-2 therapy alter homeostasis of CD4+CD25+ regulatory T cells. *Nat Med*. 2005;11(11):1238–1243.

38. Walsh PT, et al. PTEN inhibits IL-2 receptor-mediated expansion of CD4+ CD25+ Tregs. *J Clin Invest*. 2006; 116(9):2521–2531.

39. O'Gorman WE, et al. The initial phase of an immune response functions to activate regulatory T cells. *J Immunol*. 2009;183(1):332–339.

40. Feuerer M, Hill JA, Mathis D, Benoist C. Foxp3+ regulatory T cells: differentiation, specification, subphenotypes. *Nat Immunol*. 2009;10(7):689–695.

41. Rauert H, et al. Membrane tumor necrosis factor (TNF) induces p100 processing via TNF receptor–2 (TNFR2). *J Biol Chem*. 2010;285(10):7394–7404.

42. Chen X, Baumel M, Mannel DN, Howard OM, Oppenheim JJ. Interaction of TNF with TNF receptor type 2 promotes expansion and function of mouse CD4+CD25+ T regulatory cells. *J Immunol*. 2007; 179(1):154–161.

43. Belkaid Y, Rouse BT. Natural regulatory T cells in infectious disease. *Nat Immunol*. 2005;6(4):353–360.

44. O'Connor RA, Malpass KH, Anderton SM. The inflamed central nervous system drives the activation and rapid proliferation of Foxp3+ regulatory T cells. *J Immunol*. 2007;179(2):958–966.

45. McGeachy MJ, Stephens LA, Anderton SM. Natural recovery and protection from autoimmune encephalomyelitis: contribution of CD4+CD25+ regulatory cells within the central nervous system. *J Immunol*. 2005;175(5):3025–3032.

46. Almeida AR, Zaragoza B, Freitas AA. Indexation as a novel mechanism of lymphocyte homeostasis: the number of CD4+CD25+ regulatory T cells is indexed to the number of IL-2-producing cells. *J Immunol*. 2006;177(1):192–200.

47. Fontenot JD, Rasmussen JP, Gavin MA, Rudensky AY. A function for interleukin 2 in Foxp3-expressing regulatory T cells. *Nat Immunol*. 2005;6(11):1142–1151.

48. Grinberg-Bleyer Y, et al. IL-2 reverses established type 1 diabetes in NOD mice by a local effect on pancreatic regulatory T cells. *J Exp Med*. 2010;207(9):1871–1878.

49. Harnaha J, et al. Interleukin-7 is a survival factor for CD4+ CD25+ T-cells and is expressed by diabetes-suppressive dendritic cells. *Diabetes*. 2006;55(1):158–170.

50. Ito T, et al. Two functional subsets of FOXP3+ regulatory T cells in human thymus and periphery. *Immunity*. 2008;28(6):870–880.

51. Elpek KG, Yolcu ES, Franke DD, Lacelle C, Schabowsky RH, Shirwan H. Ex vivo expansion of CD4+CD25+FoxP3+ T regulatory cells based on synergy between IL-2 and 4-1BB signaling. *J Immunol*. 2007; 179(11):7295–7304.

52. Kassiotis G, Kollias G. Uncoupling the proinflammatory from the immunosuppressive properties of tumor necrosis factor (TNF) at the p55 TNF receptor level: implications for pathogenesis and therapy of autoimmune demyelination. *J Exp Med*. 2001; 193(4):427–434.

53. Liu J, et al. TNF is a potent anti-inflammatory cytokine in autoimmune-mediated demyelination. *Nat Med*. 1998;4(1):78–83.

54. McDevitt H, Munson S, Ettinger R, Wu A. Multiple roles for tumor necrosis factor–alpha and lymphotoxin alpha/beta in immunity and autoimmunity. *Arthritis Res*. 2002;4 suppl 3:S141–S152.

55. Study-group. TNF neutralization in MS: results of a randomized, placebo-controlled multicenter study. The Lenercept Multiple Sclerosis Study Group and The University of British Columbia MS/MRI Analysis Group. *Neurology*. 1999;53(3):457–465.

56. Suvannavejh GC, Lee HO, Padilla J, Dal Canto MC, Barrett TA, Miller SD. Divergent roles for p55 and p75 tumor necrosis factor receptors in the pathogenesis of MOG(35-55)-induced experimental autoimmune encephalomyelitis. *Cell Immunol*. 2000; 205(1):24–33.

57. Strom TB, Koulmanda M. Cytokine related therapies for autoimmune disease. *Curr Opin Immunol*. 2008;20(6):676–681.

58. Kirberg J, Baron A, Jakob S, Rolink A, Karjalainen K, von Boehmer H. Thymic selection of CD8+ single positive cells with a class II major histocompatibility complex-restricted receptor. *J Exp Med*. 1994; 180(1):25–34.